Biochimica et Biophysica Acta 1848 (2015) 510–517

Contents lists available at ScienceDirect

Biochimica et Biophysica Acta

journal homepage: www.elsevier.com/locate/bbamem

A thermodynamic signature of lipid segregation in biomembranes induced by a short peptide derived from glycoprotein gp36 of feline immunodeficiency virus

Rosario Oliva [a], Pompea Del Vecchio [a], Marco Ignazio Stellato [a], Anna Maria D'Ursi [b], Gerardino D'Errico [a], Luigi Paduano [a], Luigi Petraccone [a,*]

[a] Department of Chemical Sciences, University of Naples "Federico II", Naples, Italy
[b] Department of Pharmaceutical Science, University of Salerno, Fisciano, Italy

ARTICLE INFO

Article history:
Received 28 July 2014
Received in revised form 30 September 2014
Accepted 15 October 2014
Available online 23 October 2014

Keywords:
Lipid–peptide interaction
Lipid domain formation
Isothermal titration calorimetry
Differential scanning calorimetry
Model membranes
Thermodynamics

ABSTRACT

The interactions between proteins/peptides and lipid bilayers are fundamental in a variety of key biological processes, and among these, the membrane fusion process operated by viral glycoproteins is one of the most important, being a fundamental step of the infectious event. In the case of the feline immunodeficiency virus (FIV), a small region of the membrane proximal external region (MPER) of the glycoprotein gp36 has been demonstrated to be necessary for the infection to occur, being able to destabilize the membranes to be fused. In this study, we report a physicochemical characterization of the interaction process between an eight-residue peptide, named C8, modeled on that gp36 region and some biological membrane models (liposomes) by using calorimetric and spectroscopic measurements. CD studies have shown that the peptide conformation changes upon binding to the liposomes. Interestingly, the peptide folds from a disordered structure (in the absence of liposomes) to a more ordered structure with a low but significant helix content. Isothermal titration calorimetry (ITC) and differential scanning calorimetry (DSC) results show that C8 binds with high affinity the lipid bilayers and induces a significant perturbation/reorganization of the lipid membrane structure. The type and the extent of such membrane reorganization depend on the membrane composition. These findings provide interesting insights into the role of this short peptide fragment in the mechanism of virus-cell fusion, demonstrating its ability to induce lipid segregation in biomembranes.

1. Introduction

The fine interplay between lipids and proteins/peptides regulates a large number of biomembrane processes, such as molecular transport, signal reception and transduction, and membrane–membrane interactions [1–4]. However, while the effects of lipids on the peptidic counterpart have been extensively investigated (e.g., monitoring changes in conformational preferences), the role played by peptides in tuning the lipids self-organization in the bilayer is much less understood.

Among the biological processes in which biomembranes are involved, viral fusion is one of the most relevant. Enveloped viruses (e.g., influenza virus, hepatitis C virus, human immunodeficiency virus, herpes virus) possess a lipid membrane, referred to as the envelope, usually rich in sphingolipids and cholesterol [5,6]. In these cases, viral infection requires a sequence of fusion and fission events between the envelope and the target membranes for entry into the cell [7]. These energetically unfavorable processes are facilitated by the action of specific viral membrane glycoproteins that undergo conformational changes favoring micro- and mesoscopic lipid re-arrangements [8,9]. Different domains of these proteins cooperate, according to a concerted mechanism of action, in driving membrane fusion. In particular, in the case of the human immunodeficiency virus (HIV) and the feline analogue (FIV), a key role has been found to be played by the membrane-proximal external region (MPER) of the ectodomain of the respective fusion proteins, gp41 and gp36 [10,11]. Both MPER domains are unusually Trp-rich and are expected to show a marked tendency to reside at the viral envelope interface once exposed during the cascade of protein conformational changes promoting the fusion event [12].

Abbreviations: DSC, differential scanning calorimetry; ITC, isothermal titration calorimetry; CD, circular dichroism; POPC, 1-palmitoyl-2-oleoyl-sn-glycero-3-phosphocholine; POPG, 1-palmitoyl-2-oleoyl-sn-glycero-3-phosphoglycerol; DPPC, 1,2-dipalmitoyl-sn-glycero-3-phosphocholine; SM, sphingomyelin; Chol, cholesterol; MLV, multilamellar vesicles; SUV, small unilamellar vesicles; FIV, feline immunodeficiency virus; MPER, membrane proximal external region

* Corresponding author at: Department of Chemical Sciences, University of Naples "Federico II", Via Cintia, 4, I-80126, Naples, Italy. Tel.: +39 081674263; fax: +39 081674090.
E-mail address: luigi.petraccone@unina.it (L. Petraccone).

http://dx.doi.org/10.1016/j.bbamem.2014.10.017
0005-2736/

On these bases, we decided to investigate on the interaction of an octapeptide, C8 (Ac-Trp-Glu-Asp-Trp-Val-Gly-Trp-Ile-NH_2), modeled on the Trp^{770} to Ile^{777} sequence of the gp36 MPER with lipid bilayers.

Initially, we analyzed the effects of the membrane on the peptide features. Spectrofluorimetric and electron paramagnetic resonance (EPR) results showed that C8 positions at the interface of bilayers formed by glycerophosphatidylcholines [13]. The association of the peptide with the lipid membrane is driven by hydrogen bonds as well as hydrophobic interactions that the Trp side chains form with the lipid head groups, as suggested by site-directed mutagenesis studies [13] and molecular dynamics (MD) simulations [14]. Circular dichroism and NMR experiments demonstrated that, upon membrane interaction, C8 forms transient helical and turn secondary structures, in which the Trp residues assume a common orientation [14,15].

On the other hand, we focused on the changes in the bilayer microstructure induces by C8. To better explore this aspect, we considered membranes formed by various lipids, including sphingomyelin (SM) and cholesterol (Chol) [16]. It is known that these components tend to laterally segregate from glycerophospholipids, forming ordered domains, named "lipid rafts," which present reduced fluidity and permeability [17]. EPR and MD results indicated a clear preference of C8 for glycerophosphatidylcholine molecules, whose packing is significantly altered by the presence of the peptide [14,16]. This reflects in a local decrease of the bilayer thickness, while the hydration of the lipid head groups increases, as indicated by neutron reflectivity (NR) measurements.

The preferential interaction of C8 with glycerophosphatidylcholines led us to hypothesize a role played by the peptide in favoring lipid lateral segregation in mixed bilayers [16]. However, this key point deserves further investigation. In the present work, we used calorimetric (ITC) and spectroscopic techniques (CD and fluorescence) to explore the effect of membrane composition on the thermodynamics of the interaction between C8 and lipid bilayers. Further, DSC was used to evaluate the effect of C8 binding on the thermotropic behavior of the same membranes. Our results show that the thermodynamics of C8 binding is greatly affected by the composition of the membranes. Further, C8 binding induces a significant perturbation/reorganization of the lipid membrane structure. The type and the extent of such membrane reorganization is dependent on the membrane composition. These findings provide interesting insights into the role of this short fragment in the mechanism of viral envelope-cell membrane fusion.

2. Materials and methods

2.1. Materials

The peptide C8 was synthesized manually on a solid phase, using standard Fmoc/tBu chemistry, as described elsewhere [18]. Analytical RP-HPLC indicated a >97% purity level. The peptides were characterized by mass spectrometry on a Finningan LCQ-Deca ion trap instrument equipped with an electrospray source (LCQ Deca Finnigan, San José, CA, USA); samples were injected directly in the ESI source using a syringe pump at a flow rate of 5 μl/min, and spectral data were analyzed using Xcalibur software. The lipids 1-palmitoyl-2-oleoyl-*sn*-glycero-3-phosphocholine (POPC), 1-palmitoyl-2-oleoyl-*sn*-glycero-3-*rac*-phosphoglycerol (POPG), 1,2-dipalmitoyl-*sn*-glycero-3-phosphocholine (DPPC), cholesterol (Chol), and sphingomyelin (SM) were purchased from Avanti Polar Lipids Inc. (Alabaster, AL, USA) and used without further purifications. Phosphate-buffered saline (PBS) tablets were from Life Technologies Corporation. Deionized water was used for the buffer solutions and all the sample preparations.

2.2. Vesicles preparation

Appropriate amounts of lipids were weighed and dissolved in chloroform/methanol (2/1 v/v). A thin film of the lipids was produced by evaporating the solvent with dry nitrogen gas, and the sample was placed in a vacuum overnight. The sample was then hydrated with a definite amount of PBS buffer at pH 7.0 and vortexed, obtaining a suspension of multilamellar vesicles (MLV). Small unilamellar vesicles (SUV) were produced by sonication for 30 min at room temperature of multilamellar vesicles with a Sonics VCX130 (Sonics and Materials, Newtown, USA) for 30 min at room temperature. Dynamic light scattering measurements were used to check the size of the vesicles in the presence and the absence of peptide. In DLS experiments, a monochromatic light of 514 nm was used and the scattered intensity was measured at a scattering angle of 90°. The average hydrodynamic radii (R_h) of the of pure and mixed lipids vesicles (~50 nm) were consistent with the formation of unilamellar vesicles and did not change upon addition of peptide up to a peptide/lipid molar ration of 0.1. To avoid additional effects due to peptide-induced aggregation of liposomes, we did not exceed this peptide/lipid ratio in all our experiments. Liposomes with different composition were prepared: POPC alone, DPPC alone, POPC/POPG (9:1 molar ratio), POPC/SM (8:2 molar ratio), POPC/SM/Chol (6:3:1 molar ratio), and DPPC/Chol (8.5: 1.5 molar ratio).

2.3. Circular dichroism spectroscopy

Far-UV CD spectra of peptide were recorded using a JASCO J-715 spectropolarimeter (Jasco Corporation, Tokyo, Japan) as an average of 3 scans with 20 nm/min scan speed, 4 s response time, and 2 nm bandwidth, using a 0.1 cm path length quartz cuvette and at temperature of 25 °C. Typically, the peptide samples were prepared in PBS buffer solution at 35 μM concentration in the absence and in the presence of vesicles at total lipid concentration of 350 μM. For each sample, a background blank of either solvent or lipid vesicles without peptide was subtracted. An estimation of the secondary structure content was obtained from the spectra using "PEPFIT Analyses" software [19,20].

2.4. Isothermal titration calorimetry

ITC measurements were performed using a nano-ITC III (TA instruments, New Castle, DE, USA) at 25 °C. Two different titration experiments were performed: the peptide-into-lipid and the lipid-into-peptide titration [21]. In peptide-into-lipid experiment a peptide solution (30 μM) was injected in the calorimetric vessel (1 mL) containing a lipid dispersion (~5-10 mM concentration range). Under these conditions, the lipid is much in excess over the peptide during the whole titration experiment, and the injected peptide is completely bound to the membrane surface. Each injection should produce the same heat providing the binding enthalpy when divided by molarity of peptide. In the lipid-into-peptide titrations, a peptide solution (12 μM) was placed in the calorimeter cell and the lipid vesicles dispersion (10 mM) was injected in aliquots of 10 μL with 400 s intervals between the individual injections. Under these conditions, after each addition of lipid vesicles, peptide is bound and removed from bulk solution. Hence, with increasing lipid concentration in the vessel, less and less peptide is available for binding. The heat of reaction is therefore no longer constant but decreases with each lipid vesicles injection. Since the lipid-into-peptide titration leads to a complete binding of all peptide contained in the calorimetry vessel, both the total binding enthalpy and the binding isotherm can be obtained from the single experiments. In particular, the fraction of peptide bound to lipid vesicles after k injections is given by

$$\alpha^{(k)} = [PL_n]^{(k)}/P_0 = \sum_{k=1}^{k} \Delta h_k / \sum_{k=1}^{n} \Delta h_k$$

where $[PL_n]^{(k)}$ is the concentration of peptide bound after k injections, and $\sum_{k=1}^{k} \Delta h_k$ and $\sum_{k=1}^{n} \Delta h_k$ are the cumulative heat of the first k injections

and the total heat of injections, respectively. The binding isotherm was obtained by plotting the fraction of bound peptide as a function of added lipid concentration, corrected by factor $\gamma = 0.60$ [21]. The correction factor accounts for the peptide binding to be limited to the external lipid leaflet, assuming no peptide translocation through the bilayer to occur during the titration. This assumption is supported by our previous studies showing a preference of the peptide to be located at the bilayer interface [16]. The apparent binding constant K_{app} and stoichiometry (n), defined as the number of lipid molecules bound per peptide molecule, were obtained by fitting the binding isotherm with independent site binding model in the ORIGIN software package (OriginLab, Northampton, MA, USA). The binding enthalpy was obtained by dividing the total heat of injections $\sum_{1}^{n} \Delta h_k$ by the moles of peptide in the calorimetry vessel. To account for the heats of dilution in both peptide-into-lipid and lipid-into-peptide titration experiments, control experiments were performed by titrating lipid vesicles into PBS buffer solution without peptide or peptide into PBS buffer without lipid. The binding Gibbs energy and its entropic contribution were calculated using the relationships $\Delta_b G^\circ = -RT \ln K_{app}$ ($R = 8.314$ J mol^{-1} K^{-1}, $T = 298$ K) and $T\Delta_b S = \Delta_b H - \Delta_b G^\circ$.

2.5. Differential scanning calorimetry

DSC measurements were performed using a nano-DSC from TA instruments (New Castle, DE, USA). For all DSC experiments, multilamellar vesicles (MLV) were used. The excess molar heat capacity function, $<\Delta C_p>$, was obtained after a baseline subtraction, assuming that the baseline is given by the linear temperature dependence of the pretransition heat capacity. A buffer-buffer scan was subtracted from the sample scan. A volume of 300 μL of multilamellar vesicles of lipids mixtures (about 2 mM) in the absence or in the presence of peptide C8 was placed in the calorimetry vessel, and successive heating and cooling scans were performed for each sample operating at a scan rate of 1 °C/min over the temperature range of 0–60 °C. The mixtures lipid vesicles/peptide were prepared immediately before the DSC experiment, by adding the desired amount of peptide and waiting 20 min to ensure that equilibrium has been reached. The results provided here always refer to the second heating scan. DSC data were analyzed by means of the NanoAnalyze software supplied with the instrument and plotted using the Origin software package. In cases where the thermograms appeared to be a summation of overlapping components, non-linear least square curve fitting procedure supplied with Origin software was used to resolve the complex profile onto the individual components.

2.6. Fluorescence spectroscopy

The interaction of C8 with cholesterol-containing vesicles (POPC/Chol and POPC/SM/Chol) was also studied by monitoring the changes in the Trp fluorescence emission spectra of the peptide. The titrations were performed by recording the spectra of solution of peptide at fixed peptide concentration of 5 μM and lipid vesicles concentrations ranging from 0 to ~10^{-3} M.

All fluorescence spectra were recorded at 25 °C on a Fluoromax-4 fluorescence spectrophotometer (Horiba, Edison, NJ, USA), using quartz cells of 1 cm path length. The excitation wavelength was 280 nm, and the emission spectra were collected from 295 to 400 nm. The slit widths for both excitation and emission wavelengths were 5 nm.

The fraction of bound peptide at each step of titration was calculated following the changes in the fluorescence intensity at the maximum of the peptide spectrum (356 nm) using the relation

$$\alpha = \frac{I_{356} - I_{356}^{free}}{I_{356}^{bound} - I_{356}^{free}}$$

where I_{356} is the fluorescence intensity at 356 nm of peptide at different lipid concentration, I_{356}^{free} is the fluorescence intensity of the free peptide, and I_{356}^{bound} is the fluorescence intensity of the bound C8 peptide. The binding isotherms were obtained by plotting the fraction of peptide bound (α) versus lipid concentration. The apparent binding constant and stoichiometry were obtained by fitting the binding curves with an independent binding sites model implemented in the Origin software [22,23].

3. Results

3.1. Thermodynamics of C8 binding to lipid vesicles

In order to investigate the effect of the membrane composition on the C8 interaction with phospholipid bilayers, we compared the binding properties of C8 to POPC vesicles in the absence or in presence of other lipids like POPG, SM, and Chol. A small amount of negatively charged POPG lipid was added to explore the effect of the membrane surface charge density on the binding properties, whereas SM and Chol were used to mimic more closely the composition of the eukaryotic membranes. The thermodynamics of binding was determined by means of ITC measurements. ITC is the only technique that furnishes a direct measure of binding enthalpy and allows the Gibbs energy of binding to be dissected into enthalpic and entropic components [23–26].

The binding enthalpy for all the studied systems was directly measured by injecting a dilute peptide solution into the ITC cell containing a concentrated vesicles solution (peptide-into-lipid titration). Under these conditions, the lipid is much in excess over the peptide during the whole titration experiment, and the injected peptide is completely bound to the membrane surface. Fig. 1 shows the ITC traces obtained for POPC, POPC/SM, and POPC/POPG vesicles. As expected, in this conditions of high lipid/peptide (L/P) ratio, each injection produces the same heat. Similar ITC traces were obtained for all the studied systems (Figs. 1 and S1). Complete binding isotherms were obtained by a reverse titration experiments in which small amounts of a concentrated vesicles solution was injected into an ITC cell containing C8 solution (lipid-into-peptide titration). Under these conditions, each injection produces an exothermic heat of interaction, which decreases with consecutive injections. In this kind of experiments, the binding enthalpy can be evaluated by dividing the total heat generated in all the injections (cumulative heat) by the molar amount of peptide in the calorimetric cell. The binding enthalpy values were in agreement with those obtained with the peptide-into-lipid titration experiments. However, these lipid-into-peptide experiments have the advantage to generate the whole binding isotherms [21].

Fig. 2 shows the ITC traces and the corresponding binding isotherms for the reverse titration experiments performed with POPC or POPC/POPG or POPC/SM vesicles. All the binding isotherms reach a plateau value, indicating that a complete binding of the peptide to the lipid is reached at the end of the titration. However, similar experiments (lipid-into-peptide ITC titrations) performed with the cholesterol-containing membranes (POPC/Chol and POPC/SM/Chol) showed complicated ITC traces (data not shown) not suitable to generate a resolved binding isotherms. For these systems, binding isotherms derived from fluorescence titration experiments (Fig. S2) were utilized to determine the apparent binding constant (see Methods section). The thermodynamic parameters for the binding of C8 to each model membrane are summarized in Table 1. Binding of C8 to POPC, POPC/POPG, POPC/SM, and POPC/SM/Chol model membranes is both entropically and enthalpically driven, displaying a large negative change in the Gibbs energy and high binding constants (>10^6 M^{-1}).

We found that the binding enthalpy significantly changes with the lipid membrane composition. In particular, the binding enthalpy decreases in the following order: POPC/SM > POPC/POPG > POPC > POPC/SM/Chol. The entropy changes increases in the reverse order balancing the enthalpy decrease. This entropy–enthalpy compensation

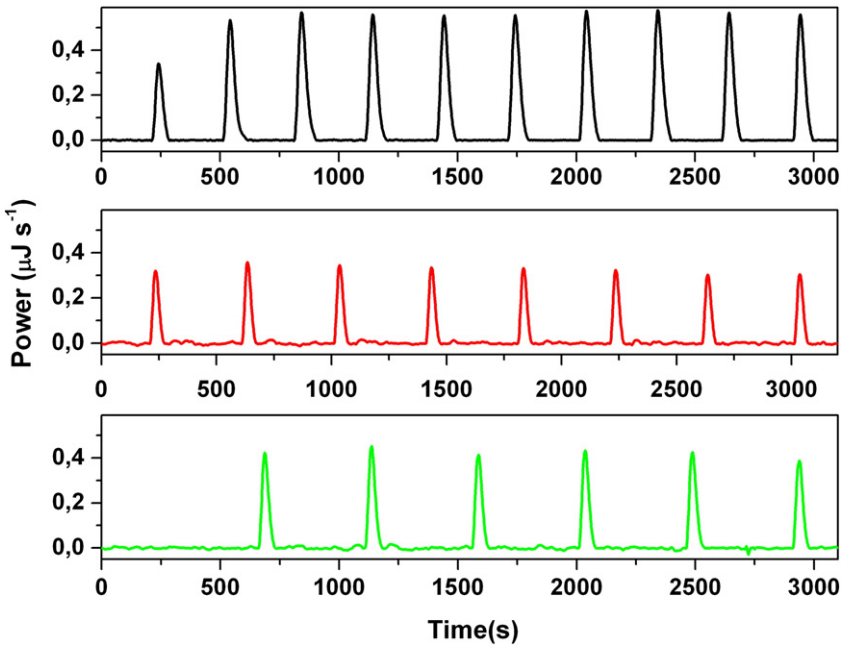

Fig. 1. ITC traces obtained from the titration of POPC (black), POPC/SM (8:2 molar ratio, red), and POPC/POPG (9:1 molar ratio, green) unilamellar vesicles (total lipid concentration 5 mM) with a C8 solution (30 μM). All experiments were carried out at 25 °C in PBS buffer.

leads to similar binding constant and Gibbs energy changes. The binding of C8 to pure POPC or POPC/SM/Chol vesicles is mostly an enthalpy-driven process whereas for the binding of C8 to the POPC/SM and POPC/POPG membranes the entropic term plays the major role in favoring the process. Among the studied membranes, the POPC/Chol is an exception. This is the only membrane that displays an unfavorable binding entropy whereas the binding enthalpy is largely favorable (−66 kJ/mol). Interestingly, C8 shows the highest binding affinity for this membrane with a K_{app} of 4×10^6 M^{-1}.

For all the studied systems, the stoichiometry values vary in the range 10–24 and represent the average number of lipid molecules involved in the interaction with C8. However, these values were not

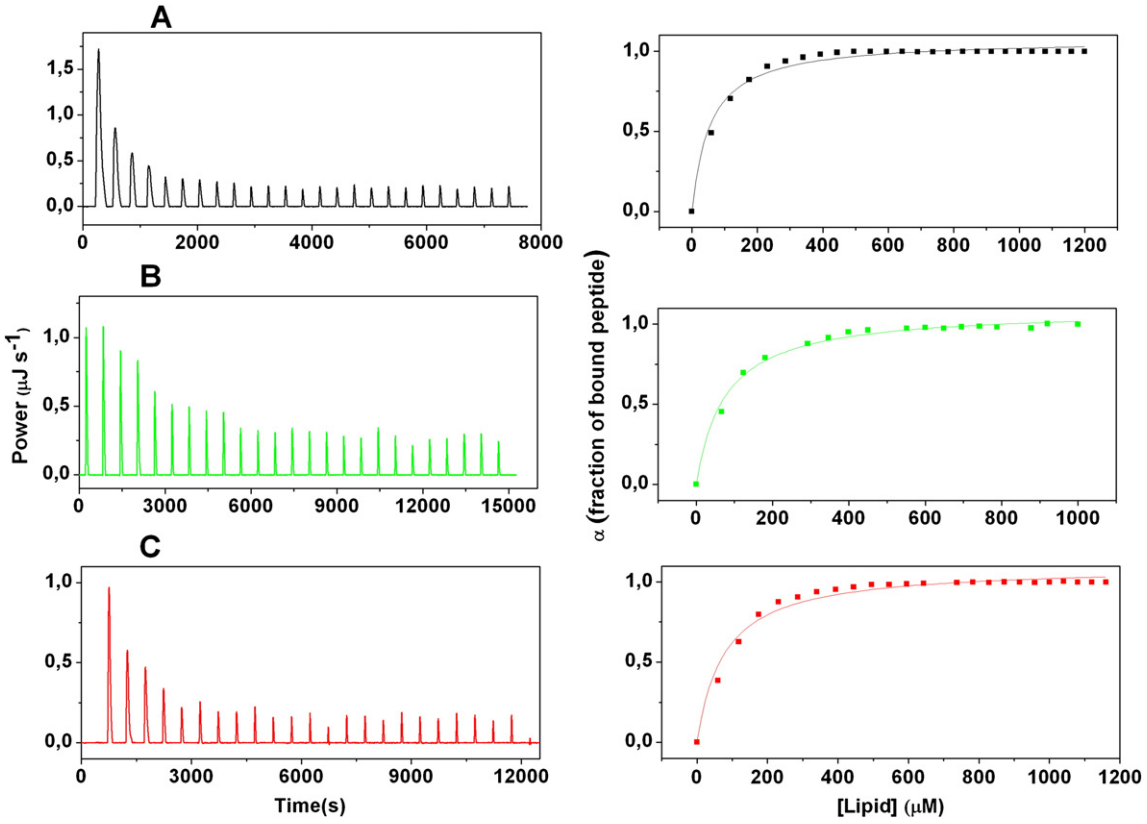

Fig. 2. ITC traces (on the left) and binding isotherms (on the right) of titration of the C8 solutions with unilamellar vesicles of (A) POPC, (B) POPC/POPG (9:1 molar ratio), and (C) POPC/SM (8:2 molar ratio). The solid lines are the best fit to the experimental data using the independent site binding model. All experiments were carried out at 25 °C in PBS buffer.

Table 1
Thermodynamic parameters of C8–liposome interactions obtained by isothermal titration calorimetry.

Lipid compositions	ΔH_b (kJ/mol)	K_{app} (M^{-1})	n	$T\Delta S_b$ (kJ/mol)	ΔG_b (kJ/mol)
POPC	−21 ± 4	(1.3 ± 0.9) × 10^6	10 ± 3	14 ± 4	−35 ± 2
POPC/POPG (9:1 mol)	−14.2 ± 1.9	(1.4 ± 0.9) × 10^6	15 ± 5	20.9 ± 2.6	−35.1 ± 1.8
POPC/SM (8:2 mol)	−10 ± 4	(1.1 ± 0.8) × 10^6	11 ± 3	25 ± 4	−35 ± 2
POPC/Chol (9:1 mol)	−66.3 ± 4.4	(4.2 ± 2.2) × 10^{6a}	24 ± 5	−28.5 ± 4.6	−37.8 ± 1.3
POPC/SM/Chol (6:3:1 mol)	−24.7 ± 1.6	(1.1 ± 0.5) × 10^{6a}	20 ± 3	9.8 ± 1.3	−34.5 ± 1.2

[a] Determined by means of fluorescence titration experiments

strictly reproducible in our experimental conditions and should be regarded as averages of broad stoichiometry ranges.

3.2. Secondary structure determination

CD spectroscopy was utilized to determine the conformation of C8 free or bound to the lipid bilayers. As the CD spectra in Fig. 3 show, C8 conformation changes significantly when liposomes are added to the peptide solution of the free C8. Analysis of the CD spectra by means of the PEPFIT analyses software shows that, in the absence of liposomes, C8 conformation is well represented by a similar amount of β-turns and unordered structures (Table 2). In contrast, a significant helical content (10–15%) was observed for C8 in the presence of POPC, POPC/SM, and POPC/POPG. These results are consistent with previous studies showing formation of secondary structures of C8 in the presence of POPC liposomes [14] or DPC micelles [15]. Due to the Chol absorbance, it was not possible to collect CD spectra for the cholesterol-containing vesicles.

3.3. Differential scanning calorimetry (DSC)

DSC experiments were performed to explore the effect of C8 binding on the thermotropic properties of the multi-component membranes. In particular, the influence of C8 binding on the thermotropic properties of DPPC, DPPC/Chol, POPC/SM, and POPC/SM/Chol vesicles was explored. DPPC was chosen to replace POPC as it has the same zwitterionic head of POPC, and at the same time, it shows a main phase transition in a temperature range suitable for DSC study. In particular, DSC profile of pure DPPC shows (Fig. 4A and Table 3) a pretransition centered at 36 °C and a main phase transition at 41.6 °C, accordingly with previously reported data [27,28]. The DSC profiles of DPPC are greatly affected by the presence of C8 (Fig. 4A), indicating that the presence of the PC zwitterionic head is a key element to determine the lipid–C8 interaction. In particular, we observed that C8 binding suppresses the DPPC pretransition and lowers the main transition peak (Fig. 4A and Table 3).

Fig. 4B shows the DSC melting profiles of the DPPC in the presence of 15% of Chol. The presence of 15% cholesterol eliminates the pretransition of DPPC and turns the peak corresponding to the main gel–liquid transition into a multicomponent DSC profile consisting of two overlapping transitions (Fig. 5A). These two components, one sharp and another broad, have been previously attributed to the melting of cholesterol-poor and cholesterol-rich domains [27,28].

The effect of C8 on the DSC profile of DPPC/Chol is shown in Figs. 4B and 5B. The inspection of the figures reveals that the C8 binding drastically changes the thermotropic behavior of DPPC/Chol. On increasing the C8 concentration, we observed a great decrease of the sharp component whereas the broad component is slightly affected (Table 4 and Fig. 5B). This result suggests that C8 preferentially binds DPPC/Chol vesicles in the cholesterol-poor domain leaving a peptide-poor Chol-enriched domain. Next, we explored the effect of the C8 binding on the thermotropic behavior of the POPC/SM vesicles. The POPC does not exhibit a phase transition above 0 °C; however, when mixed with SM, it lowers and broadens the phase transition of this lipid. In particular, we observed a broad peak centered at 15.4 °C with a transition enthalpy of 9.2 kJ/mol (Fig. 6 and Table 3). Interestingly, after addition of C8, the transition peak appears sharper and shifted at higher temperature (Fig. 6 and Table 3). This behavior is consistent with a preferential interaction of C8 with POPC lipids leading to the clustering of these lipids and to the formation of SM-enriched domain that melts at higher temperature and more cooperatively [29–31].

We finally explored the effect of the C8 binding on the thermotropic behavior of the three-component system POPC/SM/Chol (6:3:1 molar ratio). The three-component membrane has a broad phase transition around 21.5 °C, that almost disappears upon addition of C8 (Fig. 7). This behavior is also consistent with the POPC clustering induced by C8 binding and the formation of SM/Chol enriched domains [30,31]. Indeed, it is known that the presence of Chol broads the SM main transition [29]. To further check our hypothesis, we decided to determine what the transition of such an SM/Chol phase separated domain would look like by performing a DSC scan of an SM/Chol vesicles at 3:1 molar ratio. This molar ratio should correspond to the composition of the SM/Chol domain in our POPC/SM/Chol vesicle assuming complete segregation of POPC from SM and Chol. We did not observe any phase transition in such vesicles (Fig. S3). This result is consistent with the dramatic flattering of the DSC curve observed in Fig. 7 upon C8 addition and supports the hypothesis that C8 binding induces in the POPC/SM/Chol (6:3:1, molar ratio) vesicle the formation of a separate SM/Chol-enriched domain. It should be also noted that the effect of C8 on the thermotropic behavior is

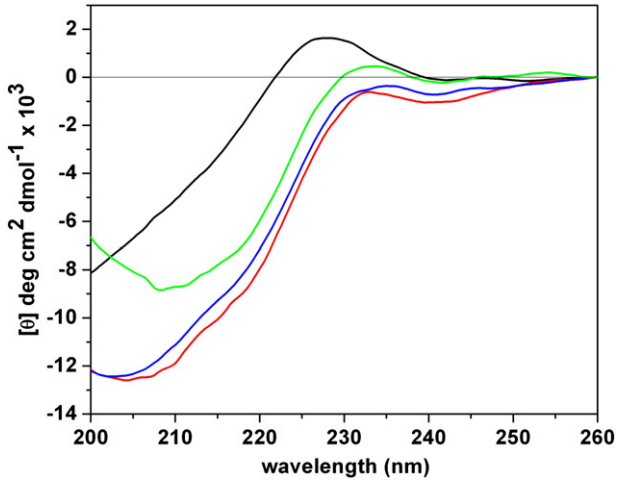

Fig. 3. Circular dichroism spectra of C8 solution (30 μM) in PBS buffer (black) and in the presence of unilamellar vesicles of POPC (red), POPC/POPG (9:1 molar ratio, green), and POPC/SM (8:2 molar ratio, blue) at lipid-to-peptide molar ratio of 10. All experiments were carried out at 25 °C in PBS buffer.

Table 2
Percentages of secondary structure elements obtained from CD spectra deconvolution of peptide C8 in the absence and in the presence of liposomes.

Lipid compositions	α-Helix	[a]β-Turn	Random coil
–		52%	48%
POPC	13%	35%	52%
POPC/POPG (9:1 mol)	10%	40%	50%
POPC/SM (8:2 mol)	11%	36%	53%

[a] This percentage is the sum of type I, II, and III β-turns.

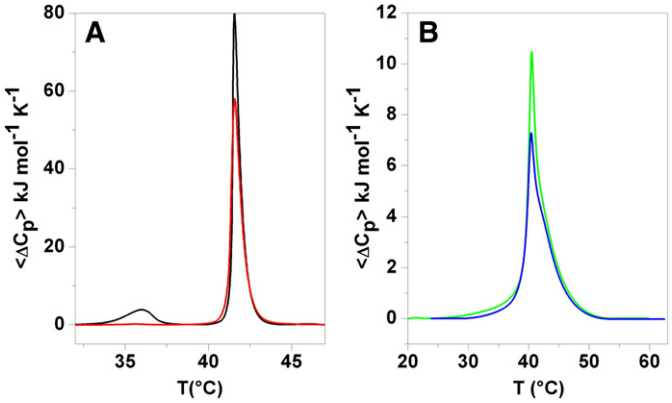

Fig. 4. (A) DSC thermograms of DPPC multilamellar vesicles in the absence (black) and in the presence (red) of C8 at the lipid-to-peptide molar ratio of 20. (B) DSC thermograms of DPPC/Chol (8.5:1.5 molar ratio) in the absence (green) and in the presence (blue) of C8 at the lipid-to-peptide molar ratio of 50.

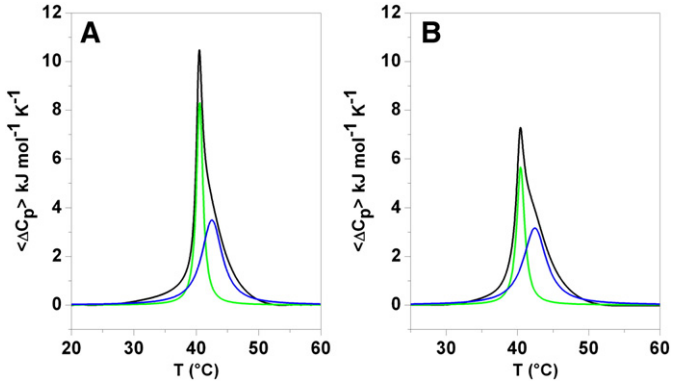

Fig. 5. Deconvolution analyses of the DSC thermograms of (A) DPPC/Chol (8.5:1.5 molar ratio) multilamellar vesicles in PBS buffer, and (B) the same multilamellar vesicles in the presence of peptide C8 at the lipid-to-peptide molar ratio of 50.

more drastic in the three components POPC/SM/Chol membrane than in the two-component POPC/SM and DPPC/Chol membranes.

4. Discussion

Previous studies have shown that C8 does not penetrate in the membrane rather it interacts with the bilayer surface and preferentially with the PC zwitterionic head [14,16]. At the same time, it was shown that the fusogenic activity of C8 is higher in mixed membranes containing also SM and Chol than that in model membrane containing only PC [16]. Further, it was suggested that the C8 fusogenic activity is related to its ability to directly alter the membrane characteristics inducing a lipids perturbation/reorganization that destabilizes the membrane and facilitates the fusion process. In this scenario, C8 binding and membrane perturbation are strictly coupled processes and should be both influenced by the membrane composition. To explore in deep details these processes, we characterized the thermodynamics of C8 interaction with several model membranes and, independently, measured the effect of C8 binding on the thermotropic behavior of the same membranes.

Our binding experiments demonstrate that the thermodynamics of C8 interaction with the lipid bilayers is significantly affected by the composition of the model membranes, such as by the surface charge density and the presence or absence of cholesterol and SM. Further, we found that the membrane reorganization upon C8 binding is different in the membrane containing separately SM and cholesterol than when they are mixed together in the same liposome. Interestingly, from the point of view of the binding affinity, we found that C8 shows similar binding Gibbs energy for pure POPC and for the two and three-component membranes, whereas, looking in details, the enthalpic and entropic contributions to the binding Gibbs energy vary significantly among the studied systems (Table 1). The binding enthalpy varies from −10 kJ/mol (for POPC/SM) to −66.3 kJ/mol (for POPC/Chol), whereas the binding entropic contribution (TΔS) varies from −28.5 kJ/mol (for POPC/Chol) to 25 kJ/mol (for POPC/SM).

Table 3
Thermodynamic parameters of the phase transitions of liposomes obtained by DSC.

Lipid compositions	T_p (°C)	ΔH_p(kJ/mol)	T_m (°C)	ΔH_m (kJ/mol)
Pure DPPC	36.0 ± 0.1	8.0 ± 0.5	41.6 ± 0.1	51.4 ± 0.5
20:1[a]			41.5 ± 0.1	47 ± 0.5
DPPC/Chol (8.5:1.5 mol)[b]			40.5 ± 0.1	38.6 ± 0.2
50:1[a]			40.4 ± 0.1	30.5 ± 0.6
POPC/SM (8:2 mol)[c]			15.4 ± 0.3	9.2 ± 0.6
20:1[a]			16.5 ± 0.3	9.7 ± 0.5
POPC/SM/Chol (6:3:1 mol)[c]			21.5 ± 0.5	4.8 ± 0.2
20:1[a]				n.d.

[a] Lipid-to-peptide molar ratio.
[b] Normalization against the mass of DPPC.
[c] Normalization against the mass of SM.

To discuss the molecular origin of such differences, it is useful to point out that ITC only measures the overall enthalpy of the binding process. This can include the following: the enthalpy of the conformational change (ΔH_{conf}) of C8, the enthalpy for the formation of new interactions (ΔH_{int}) between C8 and the membrane, the enthalpy of desolvation (ΔH_{solv}) of both C8 and membrane surfaces, and the enthalpy associated with change in the membrane structures ($\Delta H_{bilayer}$) induced by the C8 binding. Generally, the first two enthalpy changes (ΔH_{conf} and ΔH_{int}) are negative, the third term (ΔH_{solv}) is positive, and the last enthalpic contribution ($\Delta H_{bilayer}$) can be both positive or negative depending on the type and extent of the membrane reorganization process.

Our CD results have shown that changes in C8 conformation (upon binding) are small (Table 2) and will give a relatively small exothermic contribution to the overall binding enthalpy. The other two terms, ΔH_{int} and ΔH_{solv}, are probably similar for all the studied systems as it has been shown that C8 binds preferentially (with the same local interactions pattern) to the POPC lipids head group regardless the composition of each membrane [14,16]. A plausible source of the observed difference in the binding enthalpy could be the different contribution of the $\Delta H_{bilayer}$ in the two and three-component membranes compared with the pure POPC. Indeed, our DSC results have shown that C8 binding induces significant perturbation/reorganization of the lipid membrane structure. The type and the extent of such membrane reorganization depends on the membrane composition and could give different $\Delta H_{bilayer}$ contributions to the total measured enthalpy (and to the corresponding entropy) change for the binding process.

All DSC data can be rationalized assuming that the primary effect of C8 binding on the membrane organization is to segregate the POPC lipid leaving domain enriched of the other components of the membrane [30,31]. The "real" composition of these (peptide-poor) domain/s determines the observed thermotropic behavior of the liposomes. Following this hypothesis, the thermotropic behavior of the DPPC/Chol (DPPC was used to mimic POPC) liposome in the presence of C8 can be explained by the formation of Chol-enriched domain that shows the characteristic DSC profile of a DPPC liposome having a higher cholesterol content [27,28]. In other words, from the point of view of the DPPC/Chol thermotropic behavior, adding C8 has the same effect to increase the Cholesterol content. It is know that incorporation of Cholesterol in membranes results in highly ordered hydrocarbon chains [32,33]. This observation has been recently confirmed for the POPC/Chol mixtures by means of EPR measurements [16]. This ordering effect could contribute to the

Table 4
Deconvolution of DSC profiles of the DPPC/Chol liposomes in the absence and in the presence of C8.

Lipid compositions	T_m (°C) SC[b]	ΔH_m (kJ/mol) SC[b]	T_m (°C) BC[c]	ΔH_m (kJ/mol) BC[c]
DPPC/Chol (8.5:1.5 mol)	40.5 ± 0.1	17.2 ± 0.6	42.5 ± 0.1	21.7 ± 0.6
50:1[a]	40.4 ± 0.5	11.5 ± 0.7	42.4 ± 0.2	19.5 ± 0.5

[a] Lipid-to-peptide molar ratio.
[b] SC = sharp component.
[c] BC = broad component.

negative binding entropy observed for the interaction of C8 with POPC/Chol liposome (Table 1).

Regarding the POPC/SM liposome, C8 binding leads to the formation of SM-enriched domain expected to melt at higher temperature as observed in our DSC profiles (Fig. 6). Finally, in the POPC/SM/Chol membrane, C8 binding leads to the formation of SM/Chol enriched domain. Keeping in mind the low Chol content of our system, the disappearing of the mean phase transition in the POPC/SM/Chol liposome upon C8 binding suggests that POPC segregation results in an almost complete transfer of Chol in the SM enriched domain. Further, the transfer of cholesterol from POPC to SM is an exothermic process ($\Delta H = -58$ kJ/mol) [34,35]. This process is coupled to the binding process and could justify the more negative binding enthalpy observed for the three-component membrane in comparison with the pure POPC.

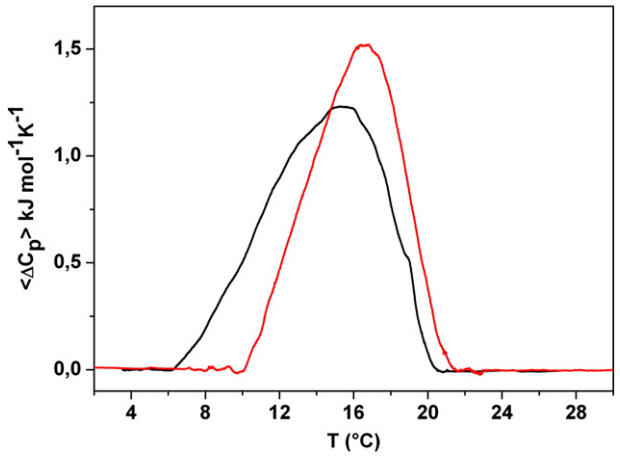

Fig. 6. DSC thermograms obtained for multilamellar vesicles composed of POPC/SM (8:2 molar ratio) in the absence (black) and in the presence (red) of C8 at the lipid-to-peptide molar ratio of 20.

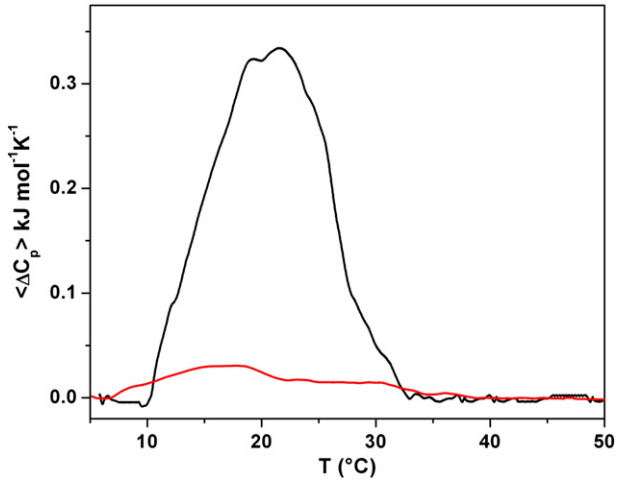

Fig. 7. DSC thermograms obtained for multilamellar vesicles composed of POPC/SM/Chol (6:3:1 molar ratio) in the absence (black) and in the presence of C8 (red) at the lipid-to-peptide molar ratio of 20.

In conclusion, our data are consistent with previous studies [14,16], indicating a specific interaction of C8 with the POPC lipids. In addition, we demonstrated that the C8 specific interaction with POPC is able to induce clustering of these lipids leading to domains formation in the membrane. These domains are enriched of all the other membrane components that do not specifically interact with the peptide. Domains formation is known to play a key role in destabilizing biological membranes and likely has a significant role in promoting the fusion process. Significantly, we found that the type and extent of domain formation and its contribution to the observed binding parameters is not correlated with C8 affinity (reflecting the binding Gibbs energy) due to the enthalpy-entropy compensation effect. All together, our results provide interesting insights into the role of this short fragment in the mechanism of viral envelope-cell membrane fusion.

Acknowledgments

This work was supported by Ministero dell'Istruzione, dell'Università e della Ricerca (MIUR, PRIN 2010–2011, Protocol Number 2010NRREPL).

Appendix A. Supplementary data

Supplementary data to this article can be found online at http://dx.doi.org/10.1016/j.bbamem.2014.10.017.

References

[1] D. Marsh, Protein modulation of lipids, and vice-versa, in membranes, Biochim. Biophys. Acta 1778 (2008) 1545–1575.
[2] O.S. Andersen, Membrane proteins: through thick and thin, Nat. Chem. Biol. 9 (2013) 664–746.
[3] S. Galdiero, A. Falanga, M. Cantisani, M. Vitiello, G. Morelli, M. Galdiero, Peptide-lipid interactions: experiments and applications, Int. J. Mol. Sci. 14 (2013) 18758–18789.
[4] A.G. Lee, Lipid–protein interactions, Biochem. Soc. Trans. 39 (2011) 761–766.
[5] B. Brugger, B. Glass, P. Haberkant, I. Leibrecht, F.T. Wieland, H.G. Krausslich, The HIV lipidome: a raft with an unusual composition, Proc. Natl. Acad. Sci. U. S. A. 103 (2006) 2641–2646.
[6] L. Kalvodova, J.L. Sampaio, S. Cordo, C.S. Ejsing, A. Shevchenko, K. Simons, The lipidomes of vesicular stomatitis virus, semliki forest virus, and the host plasma membrane analyzed by quantitative shotgun mass spectrometry, J. Virol. 83 (2009) 7996–8003.
[7] R.K. Plemper, Cell entry of enveloped viruses, Curr. Opin. Virol. 1 (2011) 92–100.
[8] A. Falanga, M. Cantisani, C. Pedone, S. Galdiero, Membrane fusion and fission: enveloped viruses, Protein Pept. Lett. 16 (2009) 751–759.
[9] S.C. Harrison, Viral membrane fusion, Nat. Struct. Mol. Biol. 15 (2008) 690–698.
[10] G. Barbato, E. Bianchi, P. Ingallinella, W.H. Hurni, M.D. Miller, G. Ciliberto, R. Cortese, R. Bazzo, J.W. Shiver, A. Pessi, Structural analysis of the epitope of the anti-HIV antibody 2 F5 sheds light into its mechanism of neutralization and HIV fusion, J. Mol. Biol. 330 (2003) 1101–1115.
[11] M. Lorizate, N. Huarte, A. Saez-Cirion, J.L. Nieva, Interfacial pre-transmembrane domains in viral proteins promoting membrane fusion and fission, Biochim. Biophys. Acta 1778 (2008) 1624–1639.
[12] W.M. Yau, W.C. Wimley, K. Gawrisch, S.H. White, The preference of tryptophan for membrane interfaces, Biochemistry 37 (1998) 14713–14718.
[13] G. D'Errico, G. Vitiello, A.M. D'Ursi, D. Marsh, Interaction of short modified peptides deriving from glycoprotein gp36 of feline immunodeficiency virus with phospholipid membranes, Eur. Biophys. J. 38 (2009) 873–882.
[14] A. Merlino, G. Vitiello, M. Grimaldi, F. Sica, E. Busi, R. Basosi, A.M. D'Ursi, G. Fragneto, L. Paduano, G. D'Errico, Destabilization of lipid membranes by a peptide derived from glycoprotein gp36 of feline immunodeficiency virus: a combined molecular dynamics/experimental study, J. Phys. Chem. 116 (2011) 401–412.

[15] M. Scrima, S. Di Marino, M. Grimaldi, F. Campana, G. Vitiello, S.P. Piotto, G. D'Errico, A.M. D'Ursi, Structural features of the C8 antiviral peptide in a membrane-mimicking environment, Biochim. Biophys. Acta 1838 (2014) 1010–1018.
[16] G. Vitiello, A. Fragneto, A. Petruk, A. Falanga, S. Galdiero, A.M. D'Ursi, A. Merlino, G. D'Errico, Cholesterol modulates the fusogenic activity of a membranotropic domain of the FIV glycoprotein gp36, Soft Matter 9 (2013) 6442–6456.
[17] L.J. Pike, The challenge of lipid rafts, J. Lipid Res. 50 (2009) S323–S328 (Suppl.).
[18] A.M. D'Ursi, S. Giannecchini, C. Esposito, M.C. Alcaro, O. Sichi, M.R. Armenante, A. Carotenuto, A.M. Papini, M. Bendinelli, P. Rovero, Development of antiviral fusion inhibitors: short modified peptides derived from the transmembrane glycoprotein of feline immunodeficiency virus, Chembiochem 7 (2006) 774–779.
[19] M.A. Amon, M. Ali, V. Bender, K. Hall, M.I. Aguilar, J. Aldrich-Wright, N. Manolios, Kinetic and conformational properties of a novel T-cell antigen receptor transmembrane peptide in model membranes, J. Pept. Sci. 14 (2008) 714–724.
[20] J. Reed, T.A. Reed, A set of constructed type spectra for the practical estimation of peptide secondary structure from circular dichroism, Anal. Biochem. 254 (1997) 36–40.
[21] J. Seelig, Titration calorimetry of lipid–peptide interactions, Biochim. Biophys. Acta 1331 (1997) 103–116.
[22] A. Cummaro, I. Fotticchia, M. Franceschin, C. Giancola, L. Petraccone, Binding properties of human telomeric quadruplex multimers: a new route for drug design, Biochimie 93 (2011) 1392–1400.
[23] L. Petraccone, I. Fotticchia, A. Cummaro, B. Pagano, L. Ginnari-Satriani, S. Haider, A. Randazzo, E. Novellino, S. Neidle, C. Giancola, The triazatruxene derivative azatrux binds to the parallel form of the human telomeric G-quadruplex under molecular crowding conditions: biophysical and molecular modeling studies, Biochimie 93 (2011) 1318–1327.
[24] J.E. Ladbury, G. Klebe, E. Freire, Adding calorimetric data to decision making in lead discovery: a hot tip, Nat. Rev. 9 (2010) 23–27.
[25] V.V. Andrushchenko, M.H. Aarabi, L.T. Nguyen, E.J. Prenner, H.J. Vogel, Thermodynamics of the interactions of tryptophan-rich cathelicidin antimicrobial peptides with model and natural membranes, Biochim. Biophys. Acta 1778 (2008) 1004–1014.
[26] A. Arouri, M. Dathe, A. Blume, The helical propensity of KLA amphipathic peptides enhances their binding to gel-state lipid membranes, Biophys. Chem. 180–181 10–21.
[27] M.G. Benesch, D.A. Mannock, R.N. Lewis, R.N. McElhaney, A calorimetric and spectroscopic comparison of the effects of lathosterol and cholesterol on the thermotropic phase behavior and organization of dipalmitoylphosphatidylcholine bilayer membranes, Biochemistry 50 (2011) 9982–9997.
[28] D.A. Mannock, R.N. Lewis, R.N. McElhaney, Comparative calorimetric and spectroscopic studies of the effects of lanosterol and cholesterol on the thermotropic phase behavior and organization of dipalmitoylphosphatidylcholine bilayer membranes, Biophys. J. 91 (2006) 3327–3340.
[29] P.R. Maulik, G.G. Shipley, N-palmitoyl sphingomyelin bilayers: structure and interactions with cholesterol and dipalmitoylphosphatidylcholine, Biochemistry 35 (1996) 8025–8034.
[30] R.M. Epand, R.F. Epand, Bacterial membrane lipids in the action of antimicrobial agents, J. Pept. Sci. 17 (2010) 298–305.
[31] R.M. Epand, R.F. Epand, C.J. Arnusch, B. Papahadjopoulos-Sternberg, G. Wang, Y. Shai, Lipid clustering by three homologous arginine-rich antimicrobial peptides is insensitive to amino acid arrangement and induced secondary structure, Biochim. Biophys. Acta 1798 (2010) 1272–1280.
[32] J.R. Silvius, Role of cholesterol in lipid raft formation: lessons from lipid model systems, Biochim. Biophys. Acta 1610 (2003) 174–183.
[33] T.P.W. McMullen, R.N.A.H. Lewis, R.N. McElhaney, Cholesterol-phospholipid, the liquid-ordered phase and lipid rafts in model and biological membranes, Curr. Opin. Colloid Interf. Sci. 8 (2004) 459–468.
[34] Z. Zhang, L. Lu, M.L. Berkowitz, Energetics of cholesterol transfer between lipid bilayers, J. Phys. Chem. 112 (2008) 3807–3811.
[35] P.F. Almeida, Thermodynamics of lipid interactions in complex bilayers, Biochim. Biophys. Acta 1788 (2009) 72–85.